Cell Cycle 13:15, 2359–2369; August 1, 2014; © 2014 Landes Bioscience

Non-muscle tropomyosin (Tpm3) is crucial for asymmetric cell division and maintenance of cortical integrity in mouse oocytes

Woo-In Jang, Yu-jin Jo, Hak-Cheol Kim, Jia-Lin Jia, Suk Namgoong*, and Nam-Hyung Kim*

Department of Animal Sciences; Chungbuk National University; Cheongju, Chungbuk, Republic of Korea

Keywords: Tropomyosin, actin, oocyte polarization, asymmetric division, cofilin

Tropomyosins are actin-binding cytoskeletal proteins that play a pivotal role in regulating the function of actin filaments in muscle and non-muscle cells; however, the roles of non-muscle tropomyosins in mouse oocytes are unknown. This study investigated the expression and functions of non-muscle tropomyosin (Tpm3) during meiotic maturation of mouse oocytes. Tpm3 mRNA was detected at all developmental stages in mouse oocytes. Tpm3 protein was localized at the cortex during the germinal vesicle and germinal vesicle breakdown stages. However, the overall fluorescence intensity of Tpm3 immunostaining was markedly decreased in metaphase II oocytes. Knockdown of Tpm3 impaired asymmetric division of oocytes and spindle migration, considerably reduced the amount of cortical actin, and caused membrane blebbing during cytokinesis. Expression of a constitutively active cofilin mutant and Tpm3 overexpression confirmed that Tpm3 protects cortical actin from depolymerization by cofilin. The data indicate that Tpm3 plays crucial roles in maintaining cortical actin integrity and asymmetric cell division during oocyte maturation, and that dynamic regulation of cortical actin by Tpm3 is critical to ensure proper polar body protrusion.

Introduction

In many living cells, the cell cortex consists of a layer of actin filaments, myosin, and actin-binding proteins.[1] The actin cortex provides the rigidity required to maintain cell integrity and shape.[2] Dynamic remodeling of the cell cortex is crucial for various cellular processes including cytokinesis, cell migration, embryogenesis, and oocyte maturation. In mammalian oocytes, the distribution of cortical actin changes during maturation and fertilization. During the first meiosis of mammalian oocytes, the meiotic spindle migrates from the center of the oocyte toward the cortex.[3] A thick F-actin cap forms in the cortex within the vicinity of the approaching meiotic spindle, and this cap marks the position of the first polar body extrusion.[4]

Various actin-binding proteins play essential roles in regulating actin filament formation and thereby help to remodel cortical actin.[5] For example, various actin nucleators belonging to the formin family as well as the Arp2/3 complex are involved in the nucleation of actin filaments at the cortex.[6,7] To generate contractile force, actin filaments in the cortex form a complex with myosin II,[8] and this actomyosin complex controls how elastic or rigid the cell cortex is.[2]

Tropomyosins are a family of coiled-coil rod-shape actin-binding proteins, and their roles in controlling the contraction of skeletal and smooth muscle have been extensively characterized.[9] In skeletal muscle, Tpm1 interacts with troponin[10] and this complex regulates the interaction between actin and myosin in response to calcium influx.[11] The interaction between caldesmon and tropomyosins regulates smooth muscle contraction.[12,13] Beside their canonical roles in skeletal and smooth muscle, various other roles of tropomyosins in non-muscle cells have recently emerged.[9] For example, tropomyosins compete with ADF/cofilin for binding to actin, and thereby protect actin filaments from depolymerization by ADF/cofilin.[14,15] Tropomyosins are essential for cytokinesis in fission yeast,[16] and knockout of the non-muscle gamma-tropomyosin (also known as Tpm3) gene causes embryonic lethality in mouse.[17,18] However, the exact roles of tropomyosins in oocyte maturation and embryogenesis are poorly understood.

In this study, we focused on the roles of Tpm3 in modulation of cortical actin during mouse oocyte maturation. By injecting small interfering RNA (siRNA) into oocytes to knockdown Tpm3, we found that Tpm3 has crucial roles in maintaining the integrity of cortical actin during oocyte maturation, and that dynamic regulation of actin by Tpm3 is critical to ensure asymmetric division, polar body protrusion, and cytokinesis.

*Correspondence to: Nam-Hyung Kim; Email: nhkim@chungbuk.ac.kr; Suk Namgoong; Email: suknamgoong@chungbuk.ac.kr
Submitted: 12/16/2013; Revised: 05/19/2014; Accepted: 05/22/2014; Published Online: 06/12/2014
http://dx.doi.org/10.4161/cc.29333

Results

The level of Tpm3 dynamically changes during mouse oocyte maturation

We investigated the mRNA and protein expression of Tpm3 in mouse oocytes. We focused on Tpm3, which is also known as gamma-tropomyosin, because this is the primary tropomyosin found at the cortex of non-muscle cells[9] and its knockout causes embryonic lethality in mouse.[17,18] Tpm3 mRNA was detected at all stages of oocyte maturation, indicating that Tpm3 is expressed during maturation of mouse oocytes (**Fig. 1A**). Next, we examined the subcellular localization of Tpm3 at different stages of meiotic maturation. At the germinal vesicle (GV) and germinal vesicle breakdown (GVBD) stages, Tpm3 was strongly detected at the oocyte cortex (**Fig. 1B**). After polar body extrusion, Tpm3 localized at the cortex, polar body, and cleavage furrow (panel MII in **Fig. 1B**), although its fluorescence intensity was markedly lower than at the GV and GVBD stages (**Fig. 1B and C**). Based on quantification of the fluorescence intensity of Tpm3 staining (**Fig. 1C**), the level of Tpm3 at the cortex significantly decreased during oocyte maturation. Actin staining (bottom panel in **Fig. 1B**) showed that the actin cap formed close to the approaching spindle in metaphase (M) I-stage oocytes, and actin was dense in the protruded polar body in MII-stage oocytes. However, the level of Tpm3 at the actin cap or polar body region did not correspond with the increased level of actin.

Knockdown of Tpm3 disrupts asymmetric division of mouse oocytes

To investigate the functional roles of Tpm3 during meiotic maturation of mouse oocytes, we injected Tpm3-targeting siRNA to knockdown Tpm3 mRNA. After microinjection of Tpm3-targeting siRNA into GV-stage oocytes, the mRNA level of Tpm3 was less than 20% of the level in control siRNA-injected oocytes (**Fig. 2A**). As shown by quantification of immunofluorescence staining with an anti-Tpm3 antibody, the protein level of Tpm3 at GV stage was significantly lower in Tpm3-targeting siRNA-injected oocytes than in control siRNA-injected oocytes (**Fig. 2C and D**).

We examined the effect of Tpm3 knockdown on maturation, polar body extrusion, and polar body size. The maturation rate of oocytes injected with Tpm3-targeting siRNA was lower than that of control siRNA-injected oocytes (42.3%, n = 267 vs. 55.1%, n = 317, $P < 0.01$). The proportion of oocytes exhibiting symmetric division or a large polar body was higher in Tpm-knockdown oocytes than in control oocytes (17.9%, n = 134 vs. 6.1%, n = 147, $P < 0.01$) (**Fig. 2B and E**). We quantified the distribution of polar body size, which was expressed as the ratio of the diameter of the polar body to the diameter of the oocyte. Tpm3 knockdown significantly increased the mean size of the polar body (Ob/Oa, where Ob is the diameter of the polar body and Oa is the diameter of the oocyte, 0.52 ± 0.024, n = 50 vs. 0.36 ± 0.009, n = 50, with a maximum value of 0.51. $P < 0.005$). Following Tpm3 knockdown, a substantial fraction of oocytes (5/50) had a 2-cell-like phenotype (**Fig. 2B and E**; **Fig. S1**), indicating that knockdown of Tpm3 significantly impairs asymmetric division of oocytes. The increased polar body size and the 2-cell-like phenotype observed in Tpm3-knockdown oocytes suggest that spindle migration was impaired. To investigate this, we examined the position of the spindle 9.5 h after siRNA injection and determined whether spindle migration was affected. While 81 ± 4% of spindles in control siRNA-injected oocytes were close to the cell cortex, the movement of 52 ± 4% of spindles in Tpm3-targeting siRNA-injected oocytes was impaired (**Fig. 2E and G**). These results suggest that Tpm3 is crucial for spindle movement during oocyte maturation.

Knockdown of Tpm3 reduces the level of cortical actin and causes membrane blebbing

Tropomyosins protect actin filaments from depolymerization by ADF/cofilin.[14,19] Therefore, we examined the intensity of actin staining in Tpm3-knockdown and control oocytes to investigate the effect of Tpm3 knockdown on cortical actin levels. The normalized fluorescence intensity of phalloidin-stained actin filaments was significantly lower in Tpm3-knockdown oocytes than in control oocytes (mean 30 ± 4, n = 17 vs. 51 ± 4, n = 26, $P < 0.005$, unit: mean pixel grayscale value (**Fig. 3A and B**), indicating that the level of cortical actin was significantly reduced after Tpm3-targeting siRNA injection. In addition, Tpm3-knockdown oocytes frequently exhibited membrane blebbing (**Fig. 3A and C**; 22.6%, n = 145), while this was not observed in any control siRNA-injected oocytes (n = 152). These results suggest that Tpm3 knockdown severely compromises the cortical integrity of the oocyte, presumably by decreasing the level of cortical actin.

To gain more insight into how Tpm3 knockdown disrupts asymmetric oocyte division and cortical membrane integrity, time-lapse imaging of maturing oocytes injected with Tpm3-targeting or control siRNA was performed. In control oocytes, spindles had migrated close to the cortex after 10 h of maturation, and polar body extrusion occurred between 11 h and 12 h (**Fig. 3D**; **Video S1**). By contrast, in Tpm3-knockdown oocytes, spindles had not reached the cortex even after 12 h, and then cytokinesis occurred, resulting in a 2-cell-like oocyte (**Fig. 3D**; **Video S2–4**). Moreover, numerous bleb-like structures formed just before cytokinesis in these oocytes (between 11 h and 20 min and 12 h and 40 min in **Fig. 3D**; **Videos S2 and S3**). In some cases, proper cytokinesis failed to occur (bottom panel of **Fig. 3D**; **Video S4**). Cytokinesis started and the cleavage furrow formed, but cytokinesis was not completed and the protruding membrane was eventually incorporated back into the oocyte, which had a 1-cell-like morphology (**Video S4**).

Knockdown of Tpm3 disrupts the cortical granule-free domain (CGFD) and the actin cap

Formation of a CGFD and actin cap near to the spindle and polar body are the main characteristics of mature mammalian oocytes.[20,21] We examined whether Tpm3 knockdown affects formation of the CGFD or the actin cap at 9.5 h after meiotic resumption. This revealed that the CGFD formed in 12 of the 13 control oocytes in which spindles migrated (**Fig. 4A and B**), whereas the CGFD failed to form in 7 of the 14 Tpm3-knockdown oocytes in which spindles migrated. Moreover, the cortical actin cap formed in 16 of the 20 control oocytes (**Fig. 4C**), while a proper cortical actin cap only formed in half (8/16) of the Tpm3-knockdown oocytes (**Fig. 4C and D**).

Overexpression of constitutively active cofilin (CA-cofilin) impairs cortical actin integrity, whereas coexpression of Tpm3 restores the level of actin

A previous study[14] suggested that one of the major roles of non-muscle Tpm is to protect actin filaments from depolymerization by ADF/cofilin. Compared with the cytoplasmic actin mesh in oocytes, which undergoes rapid polymerization and depolymerization,[22-24] cortical actin remains relatively stable during oocyte maturation, except for the formation of the cortical actin cap in the region toward which the spindle approaches.[3,25] Tpm3

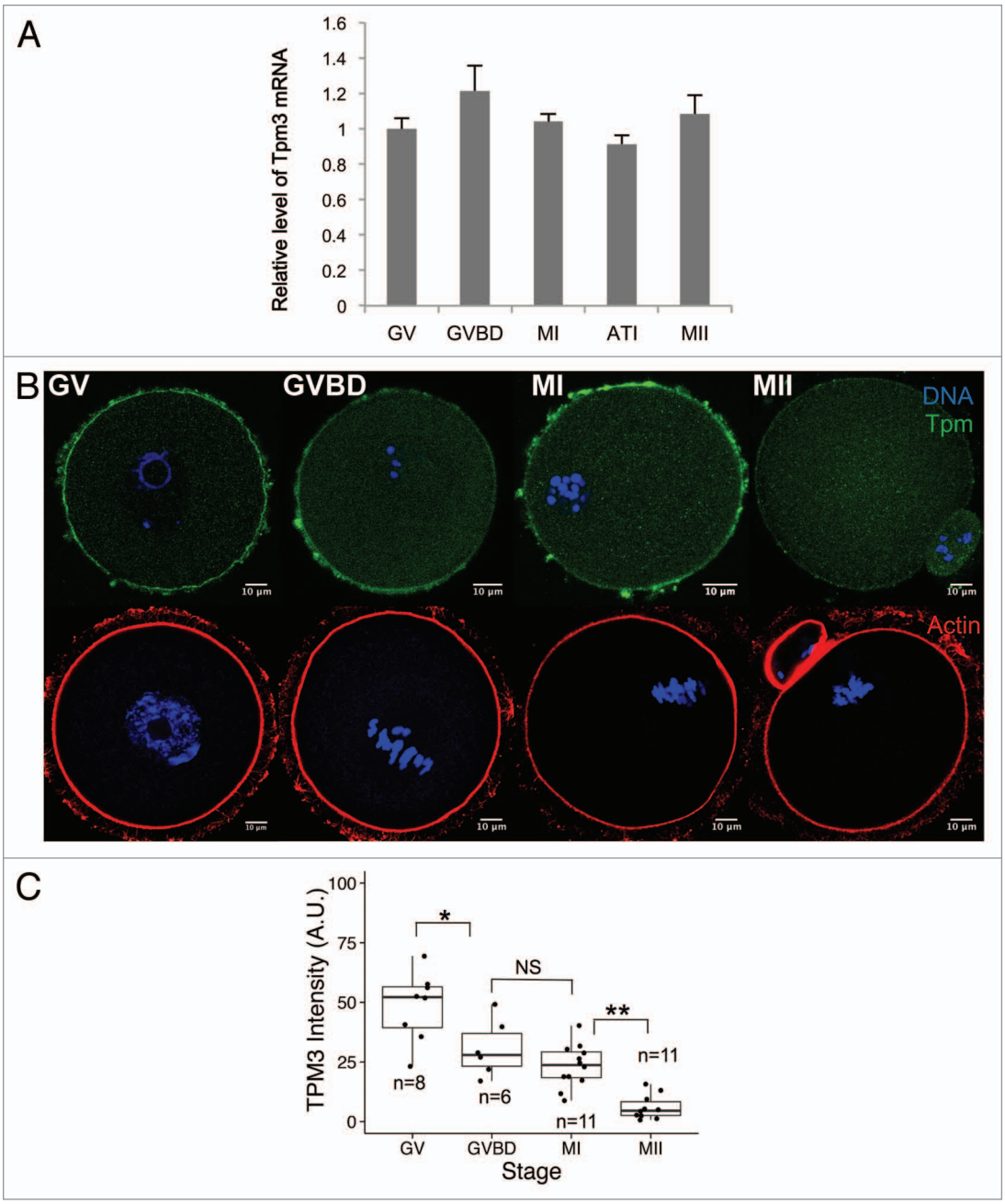

Figure 1. Dynamic changes in Tpm3 expression and localization during mouse oocyte maturation. (**A**) Quantitative PCR of Tpm3 mRNA during mouse oocyte maturation. Samples were collected after culturing for 0, 4, 8, 9.5, or 12 h, when oocytes had reached germinal vesicle (GV), germinal vesicle breakdown (GVBD), metaphase I (MI), anaphase-telophase I (ATI), and metaphase II (MII) stages, respectively. Each sample contained 20–30 oocytes. Triplicate results are expressed as the mean and SEM (**B**) Subcellular localization of Tpm3 and actin during oocyte maturation. Top: GV, GVBD, MI, and MII stages oocytes were stained with the Tpm3-specific monoclonal antibody CG3 and this is shown in green. DNA was stained with Hoechst 33342 and this is shown in blue. Bottom: Oocytes at equivalent stages were stained with phalloidin to label actin and this is shown in red. (**C**) Quantification of the intensity of Tpm3 immunostaining in the region of cortical actin. Tpm3 was stained using the monoclonal antibody CG3. The cortical localization of Tpm3 was quantitated using ImageJ and is expressed as the mean grayscale value of this fluorescence staining. Box range represents the SEM, whiskers represent the standard error, and the line inside the box represents the mean. Statistical difference was assessed by an ANOVA followed by Tukey post-hoc test. *$P < 0.05$; **$P < 0.01$; N.S., not significant.

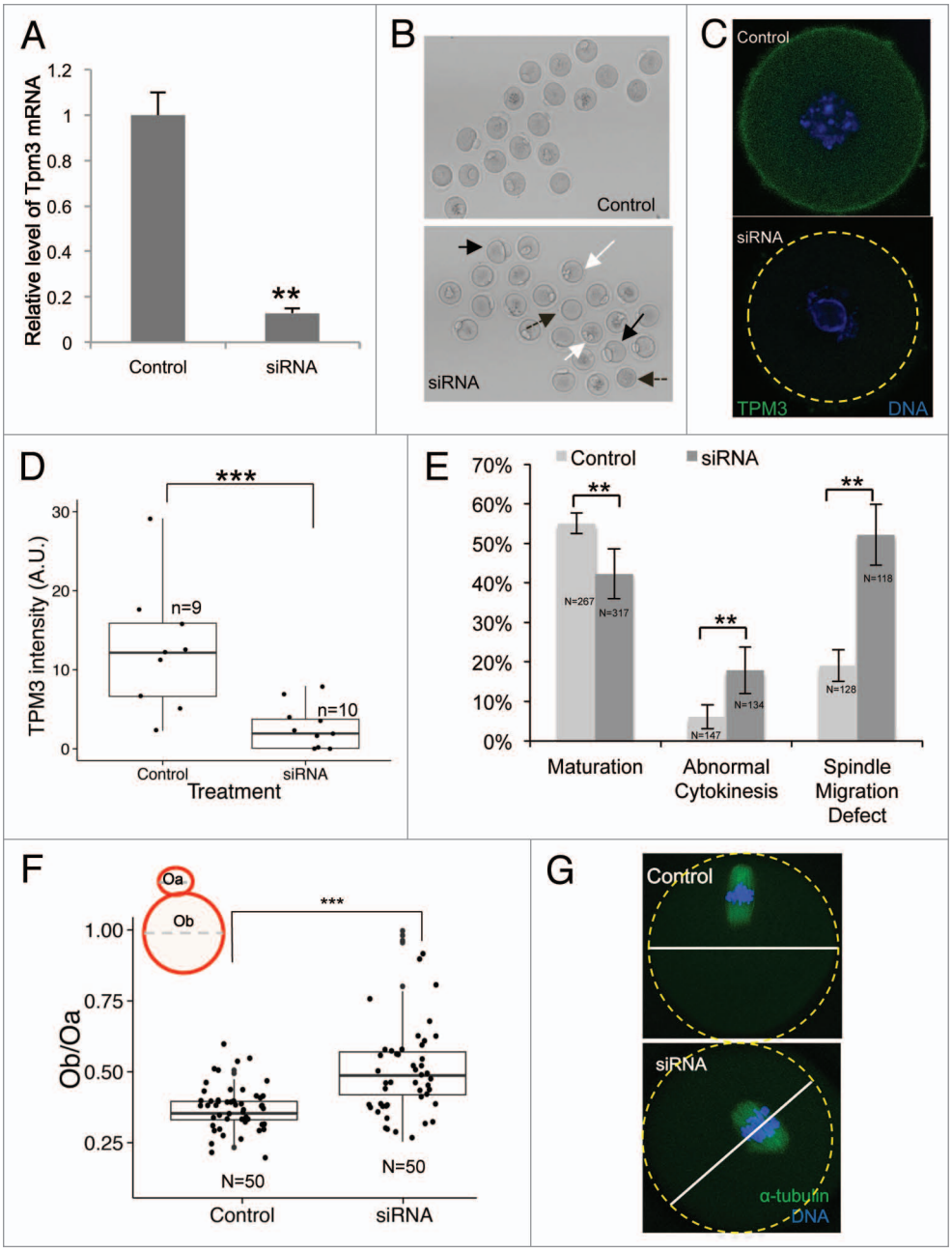

Figure 2. Knockdown of Tpm3 impairs asymmetric division of mouse oocytes. (**A**) The RNA level of Tpm3 in Tpm3-targeting small interfering RNA (siRNA)-injected oocytes (siRNA) is shown as the fraction of that in control siRNA-injected oocytes (control). (**B**) Morphology of Tpm3-targeting siRNA- or control siRNA-injected oocytes after 12 h of incubation. A large polar body (black arrow), multiple polar bodies (white arrow), and oocytes that did not form a polar body (dashed black arrow) are indicated. (**C**) Tpm3 immunostaining of control siRNA- (top) and Tpm-targeting siRNA-injected (bottom) oocytes. Green, Tpm3; blue, DNA. (**D**) Quantification of the level of cortical Tpm3 in Tpm3-targeting siRNA- and control siRNA-injected oocytes at 8 h after injection. The box range represents the standard error of the mean, whiskers represent the standard error, and the line inside the box represents the mean. Statistical significance was assessed using an ANOVA followed by Tukey post-hoc test. ***$P < 0.005$ (**E**) Percentage of MII oocytes that matured. Abnormal MII oocytes and spindle migration defects following injection of Tpm3-targeting siRNA (dark gray) or control siRNA (light gray). MII oocytes with a large polar body (diameter of the polar body larger than 50% of that of the oocyte) or a 2-cell-like morphology were considered to be abnormal. All experiments were repeated at least 3 times and involved at least 30 oocytes. The percentage of oocytes in which spindle migration was abnormal after 9.5 h of incubation is shown (n = 128 and 118 for control and Tpm3-knockdown oocytes, respectively). Statistical significance was assessed using the χ^2 test with a confidence interval of 95%. (**F**) Distribution of the ratio of the diameter of the polar body to the diameter of the oocyte in control siRNA- and Tpm3-targeting siRNA-injected oocytes. The box range represents the standard error of the mean, whiskers represent the standard error, and the line inside the box represents the mean. The statistical significance of the difference in oocyte/polar body diameter between control and Tpm3-knockdown oocytes was assessed using Welch 2-samples *t* test. ***$P < 0.005$ (**G**) Spindle location after 9.5 h of incubation. Green, α-tubulin; blue, DNA.

localized at the cortex and the amount of actin was significantly reduced in Tpm3-knockdown oocytes, which supports the idea that Tpm3 protects cortical actin from depolymerization. To test this hypothesis, we generated CA-cofilin,[26] in which the serine-3 residue was mutated to alanine, meaning that it cannot be phosphorylated by LIM kinase. This mutant was overexpressed alone or together with Tpm3 and the effects on the level of cortical actin and asymmetric division were observed.

When CA-cofilin was overexpressed by itself, the level of cortical actin was significantly decreased compared with that in control oocytes (40.8 ± 2.8, n = 24 vs. 65.0 ± 2.8 n = 15, $P < 0.05$) (**Fig. 5A and B**). The ratio of the diameter of the polar body to the diameter of the oocyte was increased by CA-cofilin expression (0.38 ± 0.02, n = 25 vs. 0.48 ± 0.02, n = 33 (**Fig. 5C**); however, when CA-cofilin was overexpressed together with Tpm3, the level of cortical actin was restored to that in control oocytes (75.0 ± 5.8, n = 30 vs. 65.0 ± 2.8 n = 15, $P = 0.4$ (**Fig. 5B**). Interestingly, the polar body enlargement induced by CA-cofilin overexpression was not restored by Tpm3 overexpression (0.48 ± 0.02, n = 33 vs. 0.54 ± 0.03, n = 27, $P = 0.23$ (**Fig. 5A and C**).

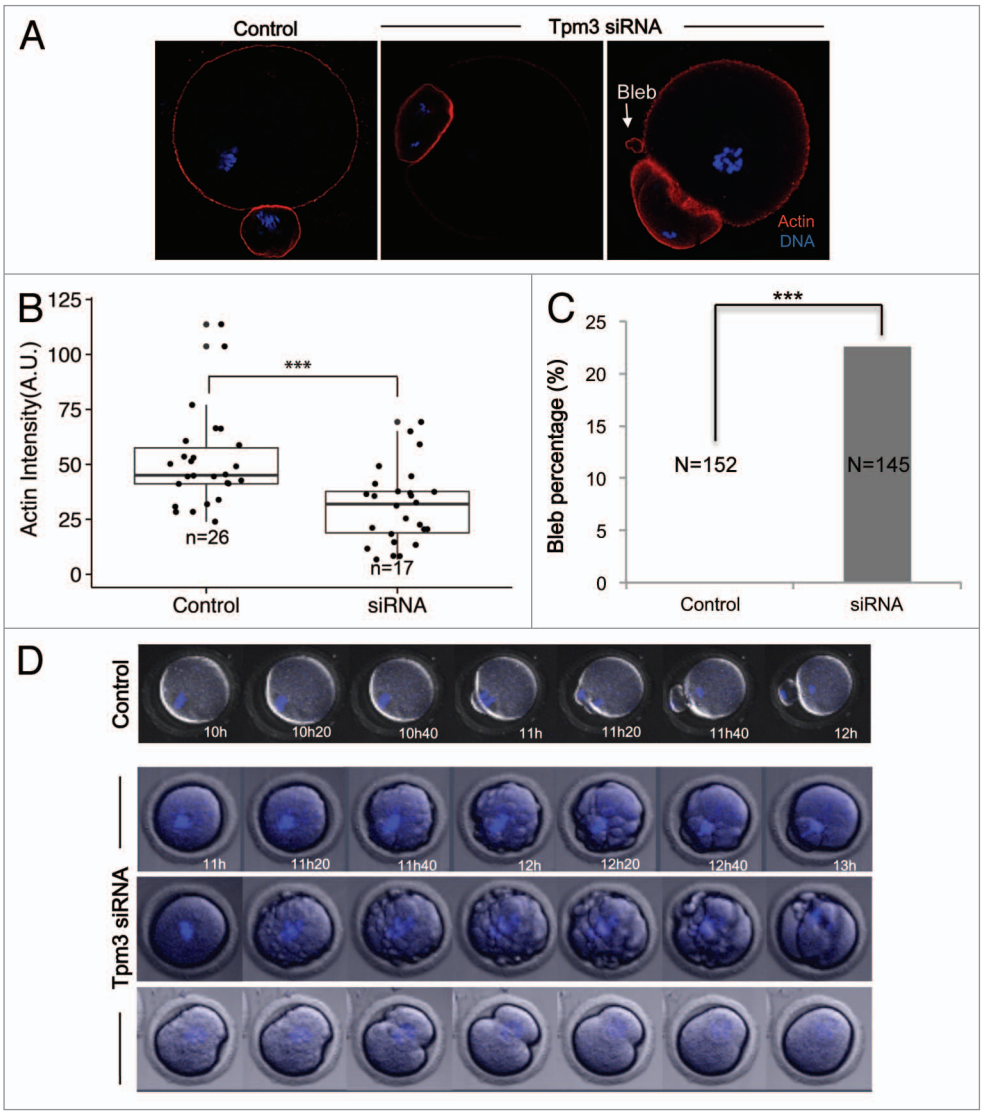

Figure 3. Knockdown of Tpm3 decreases the level of cortical actin and causes membrane blebbing. (**A**) Phalloidin staining of cortical actin in control small interfering RNA (siRNA)- and Tpm3-targeting siRNA-injected oocytes. Red, actin; blue, DNA. Arrow indicates blebs formed in Tpm3-targeting siRNA-injected oocytes. (**B**) Quantification of the amount of actin in each oocyte. The fluorescence intensity of phalloidin in the cortex of control and Tpm3-knockdown oocytes (n = 26) was measured using ImageJ and the mean value is provided. The box range represents the standard error of the mean, the whiskers represent the standard error, and the line inside the box represents the mean. Statistical significance was assessed using Welch 2-sample *t* test with a confidence interval of 95%. (**C**) Percentage of oocytes that exhibit membrane blebbing (n = 152 and 145 for control and Tpm3-knockdown oocytes, respectively). Statistical significance was assessed using the χ^2 test with a confidence interval of 95%. (**D**) Time-lapse microscopy of maturing Tpm3-knockdown oocytes. DNA was stained with Hoechst 33342 (blue). Control: control siRNA-injected oocyte. The control oocyte extruded a polar body after 11–12 h of incubation (also see **Video S1**). Tpm3-targeting siRNA: 3 representative oocytes are shown. In the top panel, numerous blebs are formed just before cytokinesis and then the polar body is extruded (also see **Video S2**). In the middle panel, the oocyte has blebs and divides symmetrically (also see **Video S3**). In the bottom panel, the oocyte divides symmetrically, but fails to finish cytokinesis (also see **Video S4**).

Discussion

In this study, we showed that Tpm3 is essential for asymmetric cell division of mouse oocytes. The roles of actin polymerization and various actin nucleators in spindle migration and asymmetric cell division in maturing oocytes have recently emerged[7,27-33]; however, the roles of other actin-binding proteins in oocyte maturation, including actin-capping proteins, ADF/cofilin, and tropomyosins, which are critical for the control of actin dynamics, are poorly understood. In this study, we present evidence that maintenance of cortical actin by Tpm3 is critical for spindle migration and polar body extrusion.

Dynamic localization of Tpm3 during oocyte maturation

Tpm3 localized at the cell cortex during oocyte maturation, indicating that Tpm3 was bound to cortical actin. Notably, the level of Tpm3 at the cortex markedly changed during oocyte maturation, being significantly lower in mature oocytes than in GV- and GVBD-stage oocytes. These findings are consistent with a previous

report that tropomyosins are barely detectable in mature, unfertilized mouse oocytes, but their levels increase after fertilization and embryo development.[34] Interestingly, the dynamic change in the distribution of Tpm3 correlates with changes in cortical stiffness during oocyte maturation[35,36] (**Fig. 6A**), implying that dynamic changes in the localization of Tpm3 at the oocyte cortex are involved in changes in cortical stiffness during oocyte maturation. It has been suggested that exclusion of myosin II from the cortex decreases cortical tension, and a previous study[15] on neuroepidermal cells showed that non-muscle Tpm can recruit myosin II to actin stress fibers. These data indicate that Tpm3 plays crucial roles in recruiting and excluding myosin II from the oocyte cortex. Therefore, removal of Tpm3 from the cortex at MII may partly underlie the exclusion of myosin II from the cortex and cortical softening; however, the detailed mechanisms and signaling pathways by which Tpm3 is removed from the cortex in MII oocytes are unclear. Given that the Mos-MAPK pathway is involved in the exclusion of myosin from the cortex at late stages of oocyte maturation,[35,37] removal of Tpm3 from the cortex may be a downstream effect of this pathway.

Considering that the level of Tpm3 was drastically reduced in MII oocytes, changes in the level of Tpm3 during oocyte maturation may be involved in fertilization. Previous studies[35,36] showed that tension in cortical membranes is decreased during maturation, and the effective tension differs between the microvillar domain to which sperm bind and fuse and the amicrovillar domain.[36] Membrane tension increases again after fertilization.[36,38,39] These results suggest that membrane tension is an important factor for controlling fertilization and, therefore, also Tpm3, and it may help to regulate fertilization via modulating cortex remodeling.

In addition to Tpm3, several tropomyosin isoforms have been characterized in non-muscle cells.[9,15,40] Tpm1, also known as α-tropomyosin,[9] is essential for embryonic development[41] and its increased expression causes defects in cytokinesis.[19] The roles of other tropomyosins, aside from Tpm3, in oocyte maturation and embryonic development are unknown. Given that non-muscle tropomyosins have non-overlapping functions,[15] the possibility that other tropomyosins play important roles in oocyte maturation cannot be excluded. For example, the level of Tpm3 immunostaining in the actin-rich cortical actin cap and the polar body regions of MII oocytes did not differ from that in other regions of the cortex, indicating that actin filaments in these regions are not coated with Tpm3. Other tropomyosin isoforms, including Tpm1 and Tpm2,[9] may be involved in the maintenance of actin filaments in these regions. In addition to Tpm3, we confirmed that Tpm1 mRNA is present in mouse oocytes using qRT-PCR (data not shown). However, detailed characterization of other tropomyosins, including Tpm1, and their functional roles remain to be performed.

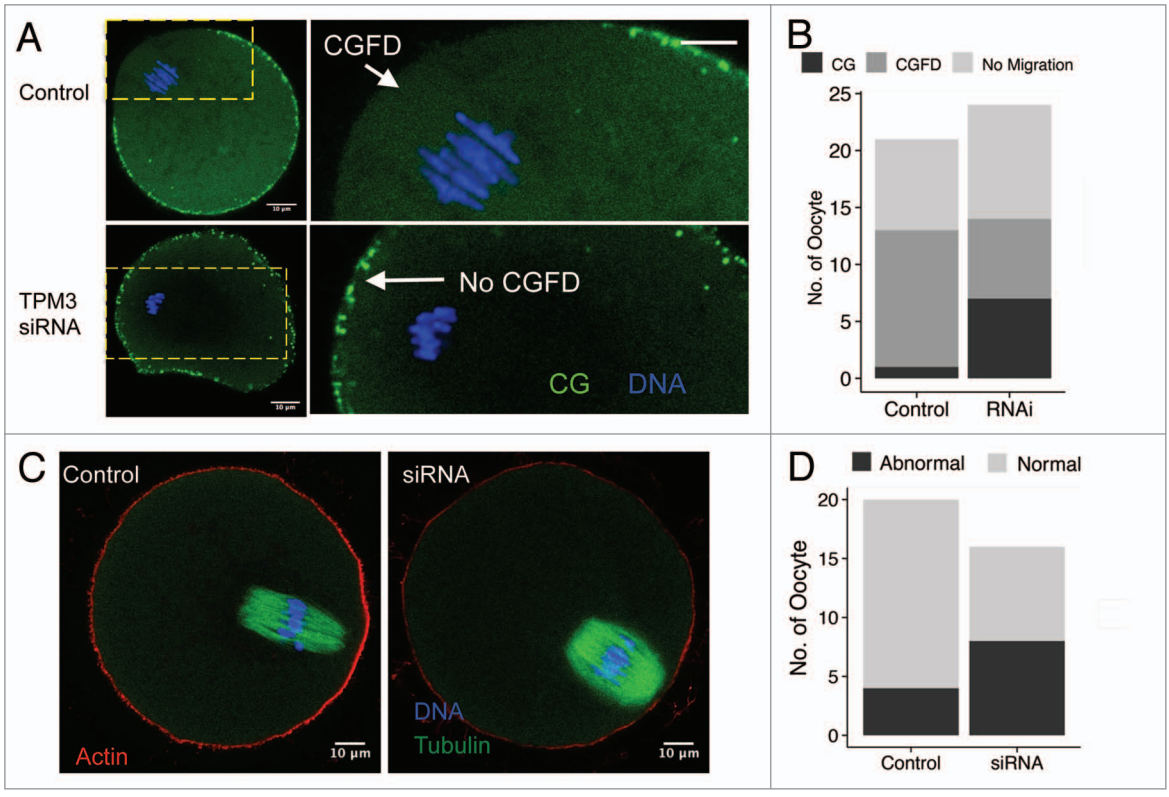

Figure 4. Knockdown of Tpm3 impairs cortical granule-free domain (CGFD) and actin cap formation in mouse oocytes. (**A**) In control small interfering RNA (siRNA)-injected oocytes, cortical granules are absent from the cortex close to where chromosomes are located during metaphase II (MII). Conversely, in Tpm3-targeting siRNA-injected oocytes, cortical granules are distributed throughout the entire cortex. Green, cortical granules; blue, DNA. (**B**) Status of CGFD formation in control siRNA-injected and Tpm3-targeting siRNA-injected oocytes. (**C**) Failure of cortical actin cap formation in Tpm3-targeting siRNA-injected oocytes.

Maintenance of cortical actin by Tpm3 and its importance in spindle migration and cytokinesis

Our knockdown experiments imply that Tpm3 functions in oocyte maturation i.e., Tpm3 protects actin filaments in the oocyte cortex during oocyte maturation. The amount of cortical actin was markedly reduced in Tpm3-knockdown oocytes. Considering the classical role of tropomyosins in protecting actin filaments from depolymerization by ADF/cofilin,[14] knockdown of Tpm3 could accelerate cortical actin depolymerization. Tpm3-knockdown oocytes displayed membrane blebbing (**Fig. 3A**), which demonstrates the importance of Tpm3 for maintaining the cortical integrity of oocytes. Membrane blebbing in the cortex is observed in oocytes that are treated with a high concentration of ethylene glycol,[42] exposed to simulated microgravity,[43] or treated with concanavalin A.[35] A recent report using fibroblasts[44] showed that laser treatment of the cortex ablates cortical actin and thereby causes bleb growth, and cortical tension mediated by actomyosin contraction causes cytoplasmic pressure, which can be reduced by bleb formation. The decreased amount of cortical actin in Tpm3-knockdown oocytes will cause local collapse of the actin network. Time-lapse imaging of Tpm3-knockdown oocytes revealed that membrane blebbing occurred just before

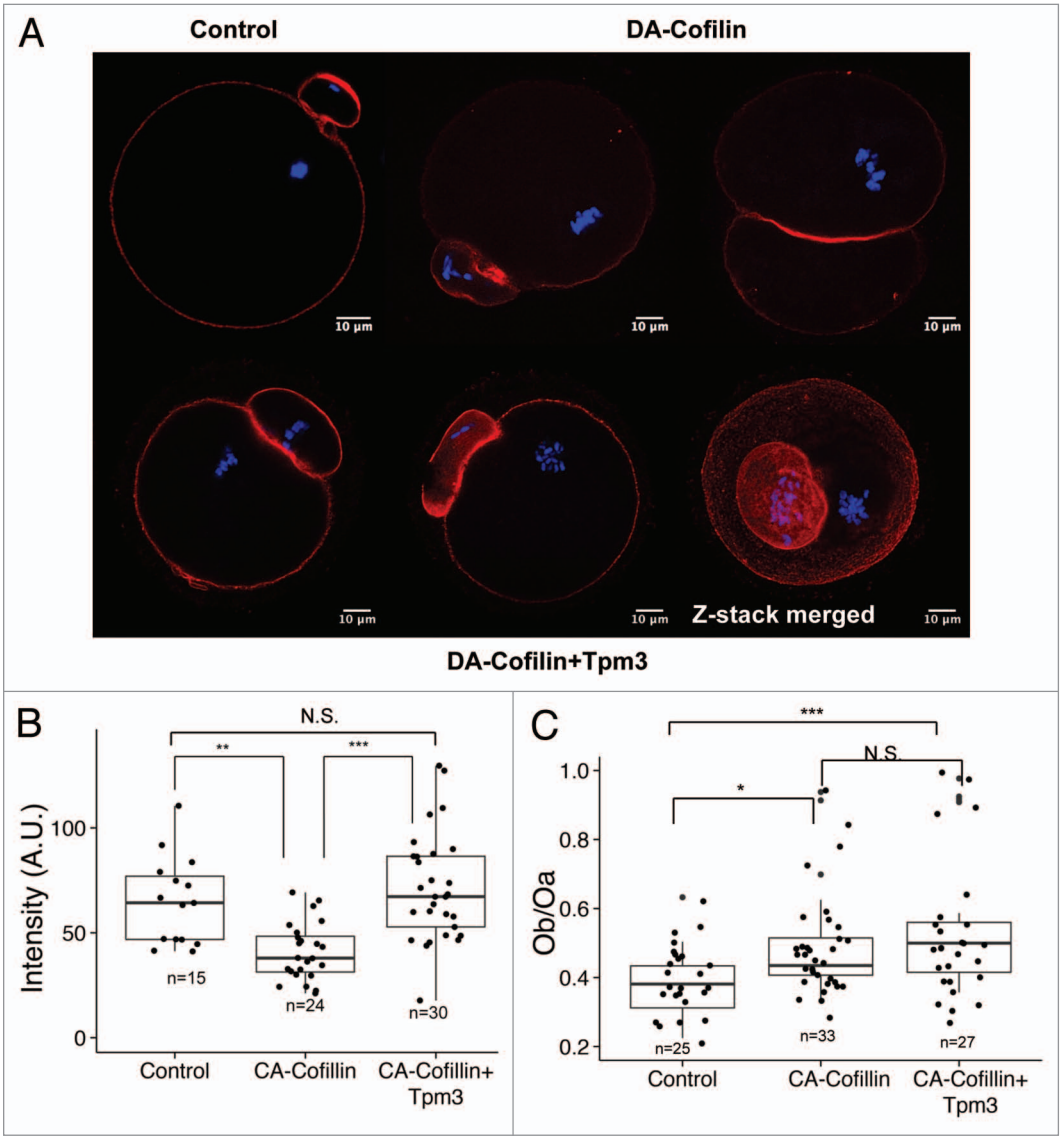

Figure 5. Tpm3 protects cortical actin from depolymerization by cofilin. (**A**) Phalloidin staining of cortical actin in oocytes injected with control small interfering RNA (siRNA), constitutively active (CA)-cofilin cRNA, or CA-cofilin and Tpm3 cRNAs. The bar represents 10 μm. Red, actin; blue, DNA. (**B**) Level of cortical actin in oocytes injected with control siRNA, CA-cofilin cRNA, or CA-cofilin and Tpm3 cRNAs. The fluorescence intensity of phalloidin staining in oocytes injected with control siRNA (n = 15), CA-cofilin cRNA (n = 24), or CA-cofilin and Tpm3 cRNAs (n = 30) were measured using ImageJ and the mean value is provided. The box range represents the standard error of the mean, the whiskers represent the standard error, and the line inside the box represents the mean. Statistical significance was assessed by an ANOVA followed by Tukey post-hoc test.*** $P < 0.005$; ** $P < 0.01$ (**C**) Distribution of the ratio of the diameter of the polar body to the diameter of the oocyte in oocytes injected with control siRNA, CA-cofilin cRNA, or CA-cofilin and Tpm3 cRNAs. The box range represents the standard error of the mean, the whiskers represent the standard error, and the line inside the box represents the mean. The statistical significance of the difference in oocyte/polar body diameter between control siRNA-injected and Tpm3-targeting siRNA-injected oocytes was assessed by Welch 2-sample *t* test. *** $P < 0.005$; * $P < 0.05$; N.S., not significant.

cleavage furrow formation (**Fig. 3D**), indicating that increased cortical tension and cytoplasmic pressure at cytokinesis is one of the causes of membrane blebbing in Tpm3-knockdown oocytes.

Tpm3 as a gatekeeper of cortical actin during oocyte maturation

Overexpression of CA-cofilin (Ser3Ala mutation) compromised cortical actin integrity, whereas overexpression of Tpm3 together with CA-cofilin restored the level of cortical actin (**Fig. 5**). These results imply that Tpm3 protects cortical actin from depolymerization by ADF/cofilin. Similar to the classical roles of tropomyosins in non-muscle cells, Tpm3-coated cortical actin filaments in oocytes should be protected from depolymerization by ADF/cofilin. As demonstrated by immunostaining and time-lapse microscopy of Tpm3-knockdown oocytes, a decreased level of actin can directly cause membrane blebbing, especially during cytokinesis (**Fig. 3D**; **Videos S2 and S3**). Laser disruption of cortical actin can induce bleb formation in somatic cells[44]; therefore, the integrity of cortical actin and of the oocyte cortex should be maintained during oocyte maturation, and one of the functions of Tpm3 may be to protect cortical actin. Interestingly, coexpression of Tpm3 did not restore the abnormal phenotype caused by CA-cofilin overexpression. While the level of cortical actin was restored by coexpression of Tpm3, the formation of large polar bodies induced by CA-cofilin expression was not suppressed by Tpm3 overexpression, suggesting that regulation of cofilin activity is crucial for asymmetric spindle migration, as shown by a recent study.[45]

In contrast to relatively stable cortical actin, the cytoplasmic actin mesh undergoes dynamic polymerization and depolymerization (**Fig. 6B**). This provides the force to maintain cytoplasmic streaming, which is suggested to directly drive asymmetric spindle migration.[3,32,46] ADF/cofilin is negatively regulated by phosphorylation at serine-3 by LIM kinase[47] and is positively regulated by dephosphorylation of this residue by the phosphatase Slingshot.[48] The activities of LIM kinases are regulated by Rho-associated kinase (ROCK),[49] which was recently reported to be involved in murine and porcine oocyte maturation.[45,50] Inhibition of ROCK causes the failure of asymmetric cell division in murine and porcine oocytes, presumably via increasing the level of active, non-phosphorylated ADF/cofilin, and these

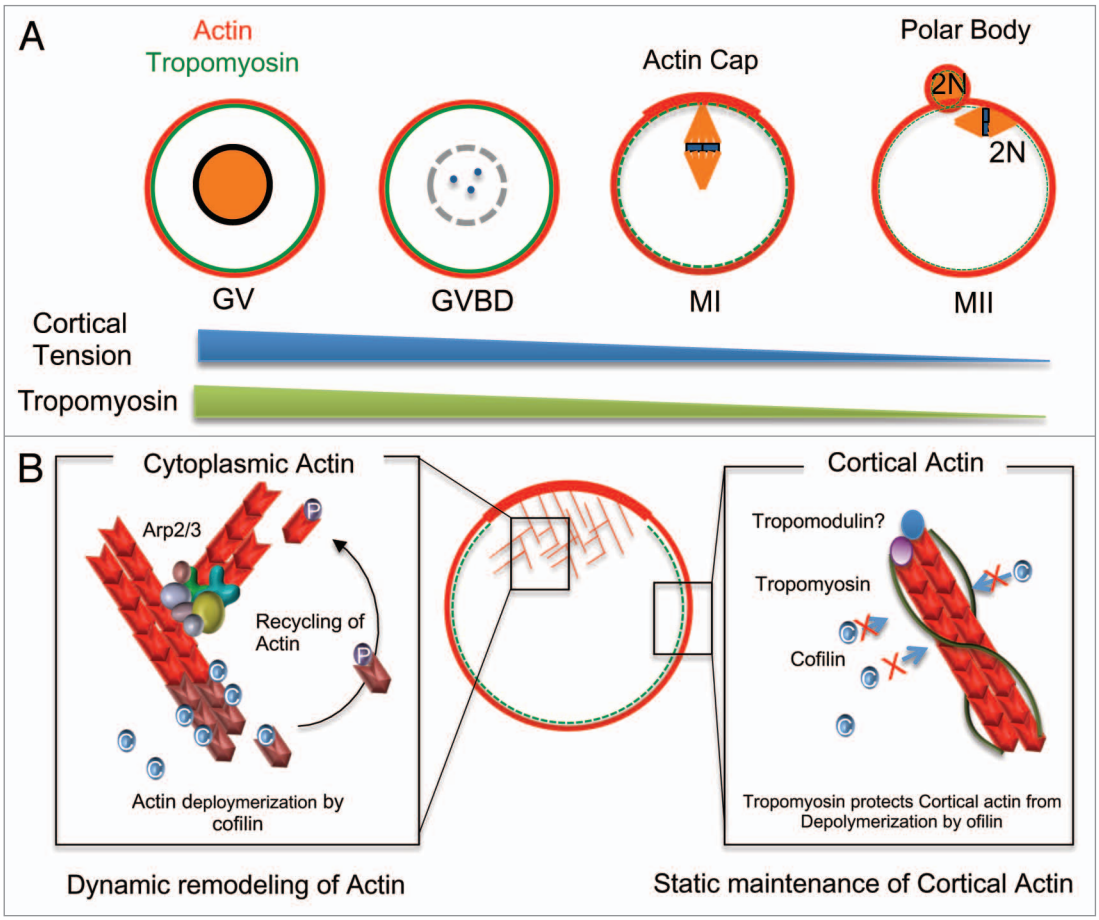

Figure 6. Roles of Tpm3 in oocyte maturation. (**A**) The localization of Tpm3 dynamically changes during oocyte maturation. At the germinal vesicle (GV) and germinal vesicle breakdown (GVBD) stages, Tpm3 colocalizes with cortical actin, whereas at the MI and MII stages, Tpm3 is excluded from the cortex. The localization of Tpm3 at the cortex correlates with recently reported changes in cortical tension.[35] (**B**) Protection of cortical actin from ADF/cofilin-induced depolymerization by Tpm3. Cytoplasmic actin in the oocyte is dynamically remodeled by polymerization induced by actin nucleators and depolymerization induced by ADF/cofilin to provide the force for cytoplasmic streaming required for spindle migration. By contrast, cortical actin is relatively stable during oocyte maturation to maintain cortical integrity. Tpm3-coated cortical actin filaments in oocytes can be protected from depolymerization induced by ADF/cofilin, as has been reported in other cells[14]

results suggest that ADF/cofilin plays a crucial role in mammalian oocyte maturation. Interestingly, the level of cortical actin is markedly decreased in ROCK-inhibited oocytes.[45,50] These data are in agreement with our finding that overexpression of CA-cofilin decreased the level of cortical actin, but that this was rescued by Tpm3 overexpression.

Conclusion

In conclusion, this study sheds light on the essential roles of Tpm3 in the maintenance of cortical actin in oocytes and of the importance of cortical integrity in spindle migration and asymmetric division. Further studies on the molecular mechanisms and signaling pathways responsible for the dynamic localization of Tpm3 will provide more insight into the roles of Tpm3 in oocyte maturation and embryogenesis.

Materials and Methods

Antibodies and chemicals

A mouse monoclonal antibody against Tpm3 (GC3)[51] was obtained from the Developmental Study Hybridoma Bank at the University of Iowa. An Alexa Fluor 488-conjugated goat anti-mouse antibody was purchased from Invitrogen. Other chemicals were obtained from Sigma, unless stated otherwise.

Oocyte collection and culture

GV-intact oocytes were collected from the ovaries of 6–8-wk-old ICR mice and were cultured in M16 medium (Sigma) under paraffin oil at 37 °C and in 5% CO_2. Oocytes were cultured for various amounts of time before immunostaining and microinjection were performed.

Real-time quantitative PCR analysis

Tpm3 gene expression was measured using real-time quantitative PCR. Total RNA was extracted from 20 oocytes using a Dynabead mRNA DIRECT Kit (Invitrogen Dynal AS). First-strand cDNA was generated using a cDNA Synthesis Kit (Takara) and Oligo(dT) 12–18 primers. A cDNA fragment of Tpm3 was amplified using the following primers: Tpm3 forward, 5′-ATCCAGCTGG TTGAAGAGGA-3′ (corresponding to 377–396 bp of NM_001253738.1), and Tpm3 reverse, 5′-CACCAACTTA CGAGCCACCT-3′ (corresponding to 594–613 bp of NM_001253738.1). Real-time PCR was performed using SYBR Green in a final reaction volume of 20 μl (qPCR kit, Finnzymes). The PCR conditions were as follows: 94 °C for 10 min, followed by 39 cycles of 95 °C for 15 s, 60 °C for 15 s, and 72 °C for 45 s, and a final extension of 72 °C for 5 min. Finally, relative gene expression was analyzed using the 2-ddCt method[52,53] by normalization to the level of mouse control mRNA. Experiments were conducted in triplicate.

siRNA injection

Approximately 5–10 pl of 50 μM Tpm3-targeting siRNA (5′-CAGCUUUGGU GUCUUUGAA (dTdT)-3′ corresponding to 1499–1517 bp of NM_001253738.1, Bioneer) was microinjected into the cytoplasm of a fully-grown GV-stage oocyte using an Eppendorf FemtoJet (Eppendorf AG) and a Nikon Diaphot ECLIPSE TE300 inverted microscope (Nikon IK Ltd) equipped with a Narishige MM0-202N hydraulic 3-dimensional micromanipulator (Narishige Inc). After injection, oocytes were cultured in M16 medium containing 2 μM milrinone for 7–8 h to ensure knockdown of *Tpm3*, washed 5 times for 2 min each with fresh M16 medium, transferred to fresh M16 medium, and cultured under paraffin oil at 37 °C in an atmosphere of 5% CO_2 in air. Control oocytes were microinjected with 5–10 pl of AccuTarget™ Control siRNA (SN-1001, Bioneer).

Overexpression of CA-cofilin and Tpm3

The open reading frames of mouse cofilin-1 and Tpm3 were amplified from cDNA prepared from GV-stage oocytes. To generate CA-cofilin-1, the serine-3 residue was mutated to alanine using PCR primers, meaning this mutant cannot be phosphorylated and inactivated by LIM kinase.[26] Amplified PCR products were subcloned into the pCS2+ vector,[54] and in vitro transcription and poly(A) tailing were performed using a SP6 mMessage mMachine Kit and a Poly-A Tailing Kit (Life Technology), respectively. Polyadenylated cofilin-S3A or Tpm3 cRNA were purified using phenol-chloroform extraction and isopropanol precipitation. cRNAs were resuspended to a concentration of 1 μg/μl in RNase-free water and injected into fully-grown GV-stage oocytes, which were cultured as described for siRNA-injected oocytes.

Immunostaining and confocal microscopy

For immunostaining of Tpm3, mouse oocytes were fixed and permeabilized in methanol at -20 °C. Alternatively, they were fixed in phosphate-buffered saline (PBS) containing 4% paraformaldehyde overnight at 4 °C, and were then transferred to membrane permeabilization solution [0.5% (v/v) Triton X-100] for 1 h. After blocking for 30 min in blocking buffer [PBS containing 1% (w/v) bovine serum albumin], oocytes were incubated overnight at 4 °C or for 4 h at room temperature with the mouse anti-Tpm3 antibody (1:50 dilution). After 3 washes with PBS containing 0.1% polyvinyl alcohol, oocytes were labeled with Alexa Fluor 488-conjugated goat-anti-mouse or rabbit-anti-goat lgG (1:100 dilution) for 1 h at room temperature. For staining with phalloidin-tetramethylrhodamine(TRITC), lectin-fluorescein isocyanate (FITC), and α-tubulin-FITC (1:200 dilution), oocytes were incubated with the stain for 1 h, washed 3 times with PBS containing 0.1% Tween 20 and 0.01% Triton X-100 for 2 min each, stained with Hoechst 33342 (10 mg/ml prepared in PBS) for 10 min, and washed 3 times in washing buffer. For staining with lectin-FITC, zona pellucida was removed with treatment of pronase as previously described.[55] Oocytes were mounted onto glass slides and examined using a confocal laser-scanning microscope (Zeiss LSM 710 META). At least 20 oocytes were examined per group. The fluorescence intensity of phalloidin-stained actin was quantified using ImageJ.[56]

Data analysis

For each treatment, at least 3 replicates were performed. Statistical analyses were conducted using Welch *t* test, Pearson chi-square test, Fisher exact test, or an analysis of variance (ANOVA) followed by Tukey multiple comparisons of means by R (R Development Core Team). Data are expressed as mean ± standard error of the mean, and $P < 0.05$ was considered significant.

Disclosure of Potential Conflicts of Interest

No potential conflicts of interest were disclosed.

Supplemental Materials

Supplemental materials may be found here:
www.landesbioscience.com/journals/cc/article/29333

Acknowledgements

This study was supported by a grant from the Next Generation Biogreen 21 Program (PJ009080 and PJ009594), RDA, Republic of Korea.

References

1. Pesen D, Hoh JH. Modes of remodeling in the cortical cytoskeleton of vascular endothelial cells. FEBS Lett 2005; 579:473-6; PMID:15642361; http://dx.doi.org/10.1016/j.febslet.2004.12.014
2. Salbreux G, Charras G, Paluch E. Actin cortex mechanics and cellular morphogenesis. Trends Cell Biol 2012; 22:536-45; PMID:22871642; http://dx.doi.org/10.1016/j.tcb.2012.07.001
3. Yi K, Li R. Actin cytoskeleton in cell polarity and asymmetric division during mouse oocyte maturation. Cytoskeleton (Hoboken) 2012; 69:727-37; PMID:22753278; http://dx.doi.org/10.1002/cm.21048
4. Maro B, Verlhac MH. Polar body formation: new rules for asymmetric divisions. Nat Cell Biol 2002; 4:E281-3; PMID:12461532; http://dx.doi.org/10.1038/ncb1202-e281
5. Pollard TD, Cooper JA. Actin, a central player in cell shape and movement. Science 2009; 326:1208-12; PMID:19965462; http://dx.doi.org/10.1126/science.1175862
6. Han Y, Eppinger E, Schuster IG, Weigand LU, Liang X, Kremmer E, Peschel C, Krackhardt AM. Formin-like 1 (FMNL1) is regulated by N-terminal myristoylation and induces polarized membrane blebbing. J Biol Chem 2009; 284:33409-17; PMID:19815554; http://dx.doi.org/10.1074/jbc.M109.060699
7. Sun SC, Wang ZB, Xu YN, Lee SE, Cui XS, Kim NH. Arp2/3 complex regulates asymmetric division and cytokinesis in mouse oocytes. PLoS One 2011; 6:e18392; PMID:21494665; http://dx.doi.org/10.1371/journal.pone.0018392
8. Cooke R. Actomyosin interaction in striated muscle. Physiol Rev 1997; 77:671-97; PMID:9234962
9. Gunning P, O'Neill G, Hardeman E. Tropomyosin-based regulation of the actin cytoskeleton in time and space. Physiol Rev 2008; 88:1-35; PMID:18195081; http://dx.doi.org/10.1152/physrev.00001.2007
10. Spudich JA, Watt S. The regulation of rabbit skeletal muscle contraction. I. Biochemical studies of the interaction of the tropomyosin-troponin complex with actin and the proteolytic fragments of myosin. J Biol Chem 1971; 246:4866-71; PMID:4254541
11. Zot AS, Potter JD. Structural aspects of troponin-tropomyosin regulation of skeletal muscle contraction. Annu Rev Biophys Biophys Chem 1987; 16:535-59; PMID:2954560; http://dx.doi.org/10.1146/annurev.bb.16.060187.002535
12. Sobue K, Sellers JR. Caldesmon, a novel regulatory protein in smooth muscle and nonmuscle actomyosin systems. J Biol Chem 1991; 266:12115-8; PMID:2061300
13. Ngai PK, Walsh MP. Inhibition of smooth muscle actin-activated myosin Mg2+-ATPase activity by caldesmon. J Biol Chem 1984; 259:13656-9; PMID:6150036
14. Ono S, Ono K. Tropomyosin inhibits ADF/cofilin-dependent actin filament dynamics. J Cell Biol 2002; 156:1065-76; PMID:11901171; http://dx.doi.org/10.1083/jcb.200110013
15. Bryce NS, Schevzov G, Ferguson V, Percival JM, Lin JJ, Matsumura F, Bamburg JR, Jeffrey PL, Hardeman EC, Gunning P, et al. Specification of actin filament function and molecular composition by tropomyosin isoforms. Mol Biol Cell 2003; 14:1002-16; PMID:12631719; http://dx.doi.org/10.1091/mbc.E02-04-0244
16. Balasubramanian MK, Helfman DM, Hemmingsen SM. A new tropomyosin essential for cytokinesis in the fission yeast S. pombe. Nature 1992; 360:84-7; PMID:1436080; http://dx.doi.org/10.1038/360084a0
17. Hook J, Lemckert F, Qin H, Schevzov G, Gunning P. Gamma tropomyosin gene products are required for embryonic development. Mol Cell Biol 2004; 24:2318-23; PMID:14993271; http://dx.doi.org/10.1128/MCB.24.6.2318-2323.2004
18. Hook J, Lemckert F, Schevzov G, Fath T, Gunning P. Functional identity of the gamma tropomyosin gene: Implications for embryonic development, reproduction and cell viability. Bioarchitecture 2011; 1:49-59; PMID:21866263; http://dx.doi.org/10.4161/bioa.1.1.15172
19. Thoms JA, Loch HM, Bamburg JR, Gunning PW, Weinberger RP. A tropomyosin 1 induced defect in cytokinesis can be rescued by elevated expression of cofilin. Cell Motil Cytoskeleton 2008; 65:979-90; PMID:18937355; http://dx.doi.org/10.1002/cm.20320
20. Liu M. The biology and dynamics of mammalian cortical granules. Reprod Biol Endocrinol 2011; 9:149; PMID:22088197; http://dx.doi.org/10.1186/1477-7827-9-149
21. Almonacid M, Terret ME, Verlhac MH. Actin-based spindle positioning: new insights from female gametes. J Cell Sci 2014; 127:477-83; PMID:24413163; http://dx.doi.org/10.1242/jcs.142711
22. Azoury J, Lee KW, Georget V, Hikal P, Verlhac MH. Symmetry breaking in mouse oocytes requires transient F-actin meshwork destabilization. Development 2011; 138:2903-8; PMID:21653611; http://dx.doi.org/10.1242/dev.060269
23. Azoury J, Lee KW, Georget V, Rassinier P, Leader B, Verlhac MH. Spindle positioning in mouse oocytes relies on a dynamic meshwork of actin filaments. Curr Biol 2008; 18:1514-9; PMID:18848445; http://dx.doi.org/10.1016/j.cub.2008.08.044
24. Schuh M, Ellenberg J. A new model for asymmetric spindle positioning in mouse oocytes. Curr Biol 2008; 18:1986-92; PMID:19062278; http://dx.doi.org/10.1016/j.cub.2008.11.022
25. Maro B, Johnson MH, Pickering SJ, Flach G. Changes in actin distribution during fertilization of the mouse egg. J Embryol Exp Morphol 1984; 81:211-37; PMID:6540795
26. Agnew BJ, Minamide LS, Bamburg JR. Reactivation of phosphorylated actin depolymerizing factor and identification of the regulatory site. J Biol Chem 1995; 270:17582-7; PMID:7615564; http://dx.doi.org/10.1074/jbc.270.29.17582
27. Leader B, Lim H, Carabatsos MJ, Harrington A, Ecsedy J, Pellman D, Maas R, Leder P. Formin-2, polyploidy, hypofertility and positioning of the meiotic spindle in mouse oocytes. Nat Cell Biol 2002; 4:921-8; PMID:12447394; http://dx.doi.org/10.1038/ncb880
28. Pfender S, Kuznetsov V, Pleiser S, Kerkhoff E, Schuh M. Spire-type actin nucleators cooperate with Formin-2 to drive asymmetric oocyte division. Curr Biol 2011; 21:955-60; PMID:21620703; http://dx.doi.org/10.1016/j.cub.2011.04.029
29. Sun SC, Sun QY, Kim NH. JMY is required for asymmetric division and cytokinesis in mouse oocytes. Mol Hum Reprod 2011; 17:296-304; PMID:21266449; http://dx.doi.org/10.1093/molehr/gar006
30. Sun SC, Xu YN, Li YH, Lee SE, Jin YX, Cui XS, Kim NH. WAVE2 regulates meiotic spindle stability, peripheral positioning and polar body emission in mouse oocytes. Cell Cycle 2011; 10:1853-60; PMID:21543895; http://dx.doi.org/10.4161/cc.10.11.15796
31. Yi K, Rubinstein B, Unruh JR, Guo F, Slaughter BD, Li R. Sequential actin-based pushing forces drive meiosis I chromosome migration and symmetry breaking in oocytes. J Cell Biol 2013; 200:567-76; PMID:23439682; http://dx.doi.org/10.1083/jcb.201211068
32. Yi K, Unruh JR, Deng M, Slaughter BD, Rubinstein B, Li R. Dynamic maintenance of asymmetric meiotic spindle position through Arp2/3-complex-driven cytoplasmic streaming in mouse oocytes. Nat Cell Biol 2011; 13:1252-8; PMID:21874009; http://dx.doi.org/10.1038/ncb2320
33. Dumont J, Million K, Sunderland K, Rassinier P, Lim H, Leader B, Verlhac MH. Formin-2 is required for spindle migration and for the late steps of cytokinesis in mouse oocytes. Dev Biol 2007; 301:254-65; PMID:16989804; http://dx.doi.org/10.1016/j.ydbio.2006.08.044
34. Clayton L, Johnson MH. Tropomyosin in preimplantation mouse development: identification, expression, and organization during cell division and polarization. Exp Cell Res 1998; 238:450-64; PMID:9473354; http://dx.doi.org/10.1006/excr.1997.3854
35. Chaigne A, Campillo C, Gov NS, Voituriez R, Azoury J, Umaña-Diaz C, Almonacid M, Queguiner I, Nassoy P, Sykes C, et al. A soft cortex is essential for asymmetric spindle positioning in mouse oocytes. Nat Cell Biol 2013; 15:958-66; PMID:23851486; http://dx.doi.org/10.1038/ncb2799
36. Larson SM, Lee HJ, Hung PH, Matthews LM, Robinson DN, Evans JP. Cortical mechanics and meiosis II completion in mammalian oocytes are mediated by myosin-II and Ezrin-Radixin-Moesin (ERM) proteins. Mol Biol Cell 2010; 21:3182-92; PMID:20660156; http://dx.doi.org/10.1091/mbc.E10-01-0066
37. Chaigne A, Verlhac MH, Terret ME. [Cortex softening: a prerequisite for the asymmetry of oocyte first division]. Med Sci (Paris) 2014; 30:18-21; PMID:24472451; http://dx.doi.org/10.1051/medsci/20143001005

38. Evans JP, Robinson DN. The spatial and mechanical challenges of female meiosis. Mol Reprod Dev 2011; 78:769-77; PMID:21774026; http://dx.doi.org/10.1002/mrd.21358
39. Kryzak CA, Moraine MM, Kyle DD, Lee HJ, Cubeñas-Potts C, Robinson DN, Evans JP. Prophase I mouse oocytes are deficient in the ability to respond to fertilization by decreasing membrane receptivity to sperm and establishing a membrane block to polyspermy. Biol Reprod 2013; 89:44; PMID:23863404; http://dx.doi.org/10.1095/biolreprod.113.110221
40. Lin JJ, Hegmann TE, Lin JL. Differential localization of tropomyosin isoforms in cultured nonmuscle cells. J Cell Biol 1988; 107:563-72; PMID:3047141; http://dx.doi.org/10.1083/jcb.107.2.563
41. Blanchard EM, Iizuka K, Christe M, Conner DA, Geisterfer-Lowrance A, Schoen FJ, Maughan DW, Seidman CE, Seidman JG. Targeted ablation of the murine alpha-tropomyosin gene. Circ Res 1997; 81:1005-10; PMID:9400381; http://dx.doi.org/10.1161/01.RES.81.6.1005
42. Hotamisligil S, Toner M, Powers RD. Changes in membrane integrity, cytoskeletal structure, and developmental potential of murine oocytes after vitrification in ethylene glycol. Biol Reprod 1996; 55:161-8; PMID:8793071; http://dx.doi.org/10.1095/biolreprod55.1.161
43. Wu C, Guo X, Wang F, Li X, Tian XC, Li L, Wu Z, Zhang S. Simulated microgravity compromises mouse oocyte maturation by disrupting meiotic spindle organization and inducing cytoplasmic blebbing. PLoS One 2011; 6:e22214; PMID:21765954; http://dx.doi.org/10.1371/journal.pone.0022214
44. Tinevez JY, Schulze U, Salbreux G, Roensch J, Joanny JF, Paluch E. Role of cortical tension in bleb growth. Proc Natl Acad Sci U S A 2009; 106:18581-6; PMID:19846787; http://dx.doi.org/10.1073/pnas.0903353106
45. Duan X, Liu J, Dai XX, Liu HL, Cui XS, Kim NH, Wang ZB, Wang Q, Sun SC. Rho-GTPase effector ROCK phosphorylates cofilin in actin-meditated cytokinesis during mouse oocyte meiosis. Biol Reprod 2014; 90:37; PMID:24429217; http://dx.doi.org/10.1095/biolreprod.113.113522
46. Yi K, Rubinstein B, Li R. Symmetry breaking and polarity establishment during mouse oocyte maturation. Philos Trans R Soc Lond B Biol Sci 2013; 368:20130002; PMID:24062576; http://dx.doi.org/10.1098/rstb.2013.0002
47. Arber S, Barbayannis FA, Hanser H, Schneider C, Stanyon CA, Bernard O, Caroni P. Regulation of actin dynamics through phosphorylation of cofilin by LIM-kinase. Nature 1998; 393:805-9; PMID:9655397; http://dx.doi.org/10.1038/31729
48. Niwa R, Nagata-Ohashi K, Takeichi M, Mizuno K, Uemura T. Control of actin reorganization by Slingshot, a family of phosphatases that dephosphorylate ADF/cofilin. Cell 2002; 108:233-46; PMID:11832213; http://dx.doi.org/10.1016/S0092-8674(01)00638-9
49. Maekawa M, Ishizaki T, Boku S, Watanabe N, Fujita A, Iwamatsu A, Obinata T, Ohashi K, Mizuno K, Narumiya S. Signaling from Rho to the actin cytoskeleton through protein kinases ROCK and LIM-kinase. Science 1999; 285:895-8; PMID:10436159; http://dx.doi.org/10.1126/science.285.5429.895
50. Zhang Y, Duan X, Xiong B, Cui XS, Kim NH, Rui R, Sun SC. ROCK inhibitor Y-27632 prevents porcine oocyte maturation. Theriogenology 2014; 82:49-56; PMID:24681214; http://dx.doi.org/10.1016/j.theriogenology.2014.02.020
51. Lin JJ, Helfman DM, Hughes SH, Chou CS. Tropomyosin isoforms in chicken embryo fibroblasts: purification, characterization, and changes in Rous sarcoma virus-transformed cells. J Cell Biol 1985; 100:692-703; PMID:2982883; http://dx.doi.org/10.1083/jcb.100.3.692
52. Livak KJ, Schmittgen TD. Analysis of relative gene expression data using real-time quantitative PCR and the 2(-Delta Delta C(T)) Method. Methods 2001; 25:402-8; PMID:11846609; http://dx.doi.org/10.1006/meth.2001.1262
53. Schmittgen TD, Livak KJ. Analyzing real-time PCR data by the comparative C(T) method. Nat Protoc 2008; 3:1101-8; PMID:18546601; http://dx.doi.org/10.1038/nprot.2008.73
54. Turner DL, Weintraub H. Expression of achaete-scute homolog 3 in Xenopus embryos converts ectodermal cells to a neural fate. Genes Dev 1994; 8:1434-47; PMID:7926743; http://dx.doi.org/10.1101/gad.8.12.1434
55. Ribas RC, Taylor JE, McCorquodale C, Maurício AC, Sousa M, Wilmut I. Effect of zona pellucida removal on DNA methylation in early mouse embryos. Biol Reprod 2006; 74:307-13; PMID:16221985; http://dx.doi.org/10.1095/biolreprod.105.046284
56. Schneider CA, Rasband WS, Eliceiri KW. NIH Image to ImageJ: 25 years of image analysis. Nat Methods 2012; 9:671-5; PMID:22930834; http://dx.doi.org/10.1038/nmeth.2089